Global and Planetary Change 162 (2018) 120–135

Contents lists available at ScienceDirect

Global and Planetary Change

journal homepage: www.elsevier.com/locate/gloplacha

Projection of future runoff change using climate elasticity method derived from Budyko framework in major basins across China

Wanqiu Xing[a,b], Weiguang Wang[a,c,*], Shan Zou[d], Chao Deng[a,c]

[a] State Key Laboratory of Hydrology-Water Resources and Hydraulic Engineering, Hohai University, Nanjing 210098, China
[b] School of Earth Sciences and Engineering, Hohai University, Nanjing 211100, China
[c] College of Water Resources and Hydrology, Hohai University, Nanjing 210098, China
[d] Bureau of Hydrology of Changjiang Water Resources Commission, Wuhan 430010, China

ARTICLE INFO

Editor: Dr. Matenco Liviu

Keywords:
Climate elasticity
Budyko framework
Runoff change
Future projection
China

ABSTRACT

This study established a climate elasticity method based on Budyko hypothesis and enhanced it by selecting the most effective Budyko-type formula to strengthen the runoff change prediction reliability. The spatiotemporal variations in hydrologic variables (i.e., runoff, precipitation and potential evaporation) during historical period were revealed first and the climate elasticities of runoff were investigated. The proposed climate elasticity method was also applied to project the spatiotemporal variations in future runoff and its key influencing factors in 35 watersheds across China. Wherein, the future climate series were retrieved by consulting the historical series, informed by four global climate models (GCMs) under representative concentration pathways from phase five of the Coupled Model Intercomparison Project. Wang-Tang equation was selected as the optimal Budyko-type equation for its best ability in reproducing the runoff change (with a coefficient of determination and mean absolute error of 0.998 and 1.36 mm, respectively). Observed runoff presents significant decreasing trends in the northern and increasing trends in the southern regions of China, and generally its change is identified to be more sensitive to climatic variables in Hai River Basin and lower Yellow River Basin. Compared to the runoff during the reference period, positive change rates in the north and negative change rates in the south of China in the mid-21st century can be practically generalized from the majority of GCMs projections. This maybe resulted from the increasing precipitation, especially in parts of northern basins. Meanwhile, GCMs project a consistently upward trend in potential evaporation although significant decreasing trends occur in the majority of catchments for the historical period. The results indicate that climate change will possibly bring some changes to the water resources over China in the mid-21st century and some countermeasures of water resources planning and management should be taken.

1. Introduction

The warming occurred in recent decades and the warming trends will unambiguously continue, due to anthropogenic net increases in atmospheric greenhouse gas concentrations (IPCC, 2013). Associated with global surface warming, changes in mean precipitation across many regions have also been documented due to the increasing atmospheric moisture content (Wang et al., 2013a). One of the most significant potential consequences of climate change may be the ongoing intensifications in regional hydrological cycles. As the most important component of hydrological cycle, runoff determines the available water for irrigation, domestic water and hydroelectric generation and is directly related to the human beings. In-depth understanding of the impacts of climate change on runoff is hence of great significance for effective water resources analysis, management, and policy formulation. Therefore, investigation on the responses of runoff to climate change, especially the future projection of runoff, have recently drawn considerate concerns (e.g., Teng et al., 2012; Vetter et al., 2017).

To assess the possible future changes in regional hydrologic cycles and water availability, hydrological models with climate outputs from the global climate models (GCMs) driven by greenhouse gas emission scenarios are usually employed. In despite of being good at characterizing more precise spatial and temporal patterns with the information of soil and vegetation, the physically based hydrological models are always subject to the requirement of large data sets (e.g., topography, vegetation and soil data) (Thompson et al., 2013), time-consuming calibration and validation process (Mishra et al., 2010), and high uncertainties in the model structure and parameter estimation (Wang

* Corresponding author at: State Key Laboratory of Hydrology-Water Resources and Hydraulic Engineering, Hohai University, Nanjing 210098, China.
E-mail addresses: wangweiguang006@126.com, wangweiguang@hhu.edu.cn (W. Wang).

https://doi.org/10.1016/j.gloplacha.2018.01.006
Received 23 September 2017; Received in revised form 23 November 2017; Accepted 8 January 2018
Available online 13 January 2018
0921-8181/ © 2018 Elsevier B.V. All rights reserved.

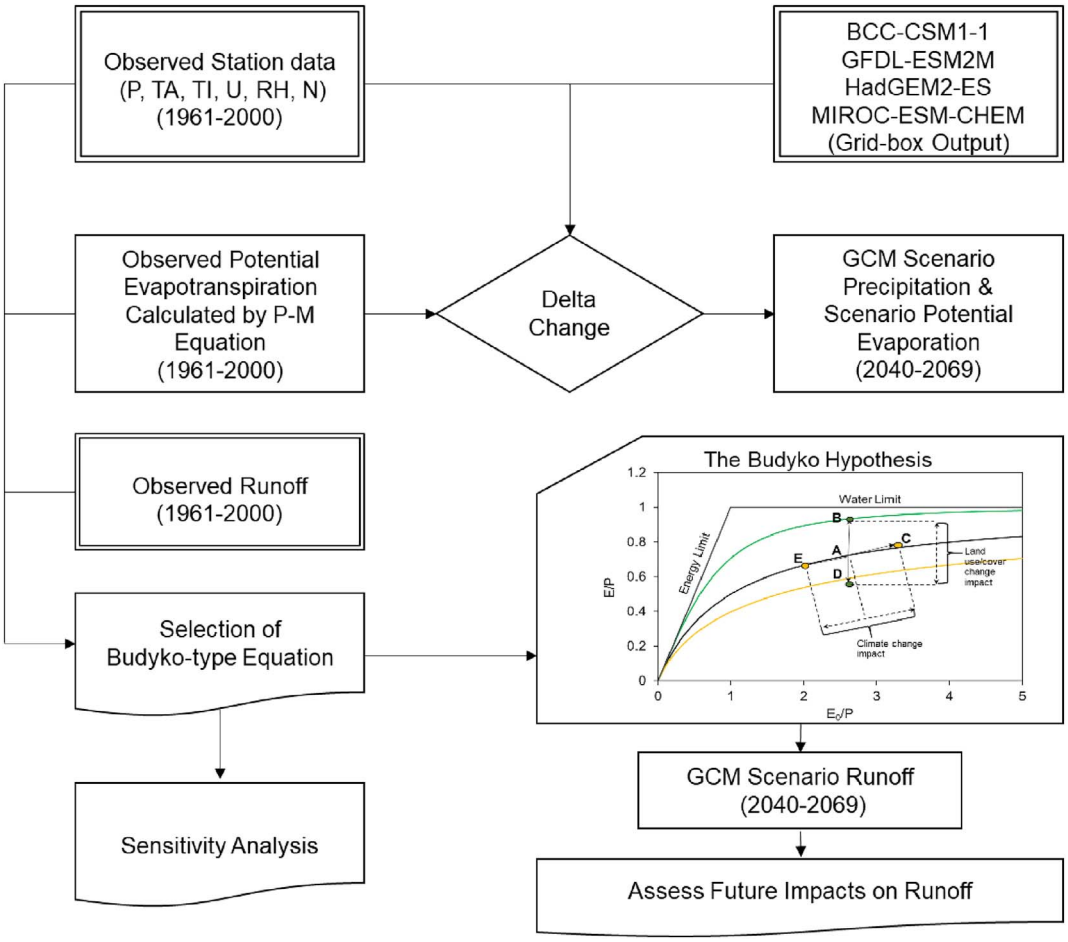

Fig. 1. An overview of the datasets, procedures, and models used in the study.

et al., 2013a). While the climatic elasticity methods, which are comparable to more complex hydrological modeling approaches for evaluating climate change impact on the long-term streamflow changes (Teng et al., 2012), have been widely used to assess climate change impact on streamflow (Renner et al., 2012; Huang et al., 2016; Kumar et al., 2016; Wang et al., 2016).

A simple first-order theoretical equation to describe the water and energy balance, proposed by Budyko (1974) has been found wide applications and experienced a revival in understanding of hydrologic behaviors under changing environments (e.g., Milly, 1994; Choudhury, 1999; Roderick and Farquhar, 2011; Williams et al., 2012; Xu et al., 2013; Greve et al., 2015; Singh and Kumar, 2015; Zhang et al., 2016b). Through the Budyko equation, the partitioning of precipitation (P) into evapotranspiration (E) and runoff (Q) at mean annual catchment scales is governed to first-order by the competition between water supply and energy availability in despite of the complicated interactions among climate (Berghuijs et al., 2014), soil (Donohue et al., 2012), topography (Shao et al., 2012) and vegetation (Li et al., 2013). Recently, Wang et al. (2016) developed an analytical derivation of multiple elasticities based on Budyko and Penman frameworks, and preliminarily assessed its applicability. The results indicate that if the overall climatic effect is of interest, the two-parameter elasticity method should be adopted with a higher confidence in capturing the runoff change as a whole, while the multiple-parameter elasticity method should be chosen if the further separating climate effect on runoff is of interest.

Significantly influenced by the monsoon, the mean annual runoff of the primary seven large river basins across China account for 73.8% of the whole China. These basins play an important role in the sustainable development of economy and ecology with hosting more than 90% of the population and accounting for nearly 96% of GDP in China (China, 2009). Over the past several decades, the water-energy balance and climatic conditions in China have experienced significant changes. Recently, strong warming, uneven regional precipitation change patterns, and periodic fluctuation of reference evapotranspiration have been reported in numerous studies (e.g., Sun et al., 2016; Wu et al., 2016; Xing et al., 2016). Therefore, there is a growing need to investigate the response of future runoff change to climate change in these basins for offering the regional strategy for water resource and eco-environment management. However, the land surface characteristics of the seven large river basins, including vegetation, topography and soil properties vary significantly, leading to the differences in mechanism of runoff generation and flow concentration. Moreover, most of aforementioned efforts of employing Budyko framework focused only on identifying the contribution of historical climate change and human activities on runoff change. Report on projection of future runoff under climate change with Budyko framework is very limited. Even that in the available literature on modeling future runoff involved Budyko hypothesis (e.g., Teng et al., 2012; Meng and Mo, 2012; Guo et al., 2015), most of them used methods derived from non-parametric Budyko-type equations or the form of Budyko-type equations prototype. The non-parametric Budyko-type equations cannot reflect the differences of vegetation, soil types and topography information across various catchments represented by the shape parameter. Besides, with only providing the value of mean annual runoff in a given climatic condition, the Budyko-type equation prototype cannot estimate the response of runoff to the change of climatic input.

Therefore, the overall objective of this study is: (1) to detect and compare the applicability of the universal functional forms in Budyko

framework for the study area and then seek out an optimal Budyko-type equation for modeling runoff change over major basins across China; (2) to conduct a comprehensive investigation on how the runoff response to precipitation and potential evaporation with the selected Budyko equation; and (3) to further predict future spatiotemporal changes in runoff during mid-21st century using climate elasticity method, where the future climatic data is obtained from four calibrated GCMs and four representative concentration pathways from phase five of the Coupled Model Intercomparison Project. An overview of the datasets, procedures and models is given in the flowchart presented in Fig. 1.

2. Study area and data processing

2.1. Study area

This study synthesized quantitative assessments of runoff change response to climate change for 35 watersheds across China. Whereas the watersheds were collected from seven large river basins, including the Songhua River Basin, the Liao River Basin, the Hai River Basin, the Yellow River Basin, the Huai River Basin, the Yangtze River Basin, and the Pearl River Basin (see Fig. 2). The mean annual runoff of seven large rivers account for 73.8% of the total water resources in China. As affected by the topography and climate, the rivers are distributed unevenly over regions. The runoff depth of the natural river, which depends on precipitation, evapotranspiration and physical characteristics of watersheds, gradually descends in magnitude from the south towards the north. It is greater than 1000 mm in some southeastern regions and less than 20 mm in some northern regions (see Table 1). A strong warming of China with 1.44 °C increase in mean temperature (Sun et al., 2016). Change in precipitation of China exhibits distinctive regional patterns with receiving less and less precipitation in western China and experiencing more rainfall in eastern China (Wu et al., 2016). Dominated by the episodic dynamics of the ocean–atmosphere interaction in earth, reference evapotranspiration generally presents decadal variations rather than monotonic response to climate change reported in previous studies (Xing et al., 2016). Also considering the crucial role of the seven large river basins in society and economy, the analysis of fluvial hydrological response to climate variability in these basins is of great importance for understanding watershed hydrology and improving water resources management practice.

2.2. Hydrological data

Annual runoff (Q) of 35 watersheds from 1961 to 2000 was acquired from the Ministry of Water Resources, China. The quality of the hydrological data was firmly controlled before its release. The missing data accounted for less than 1% of the total data and were processed using the 11-year moving average method. The basic information (including longitude, latitude and the drainage area) of each hydrological station is displayed in Table 1.

2.3. Climate data

In this study, two sets of climate data were used to investigate the responses of runoff to climate change, including historical meteorological data (i.e., observed station data), and future climate projections from GCMs.

Daily meteorological variables, including precipitation, air temperature, sunshine duration, wind speed, and relative humidity collected from total 195 meteorological stations for the period 1961–2000 were provided by the National Climatic Center of the China Meteorological Administration (http://cdc.nmic.cn). Potential evaporation (E_0) was estimated using the Penman method (Penman, 1948), which has been shown to be the most optimal formula to capture climate change (Liu and McVicar, 2012). Details of the catchment average P and E_0 calculation can be found by Yang and Yang (2011). The location of the seven major basins and the distribution of hydrological and meteorological stations over these basins are shown in Fig. 2.

The future climate projections were acquired from four GCMs including BCC-CSM1.1, MIROC-ESM-CHEM, GFDL-ESM2M and HadGEM2-ES (the detailed description can be seen in Table 2), participating in the Coupled Model Intercomparison Project Phase 5 (CMIP5) experiment. These four models were selected since they were widely applied in climate impact studies with favorable feasibility in China (Guo et al., 2015; Yin et al., 2015). The projected changes for a

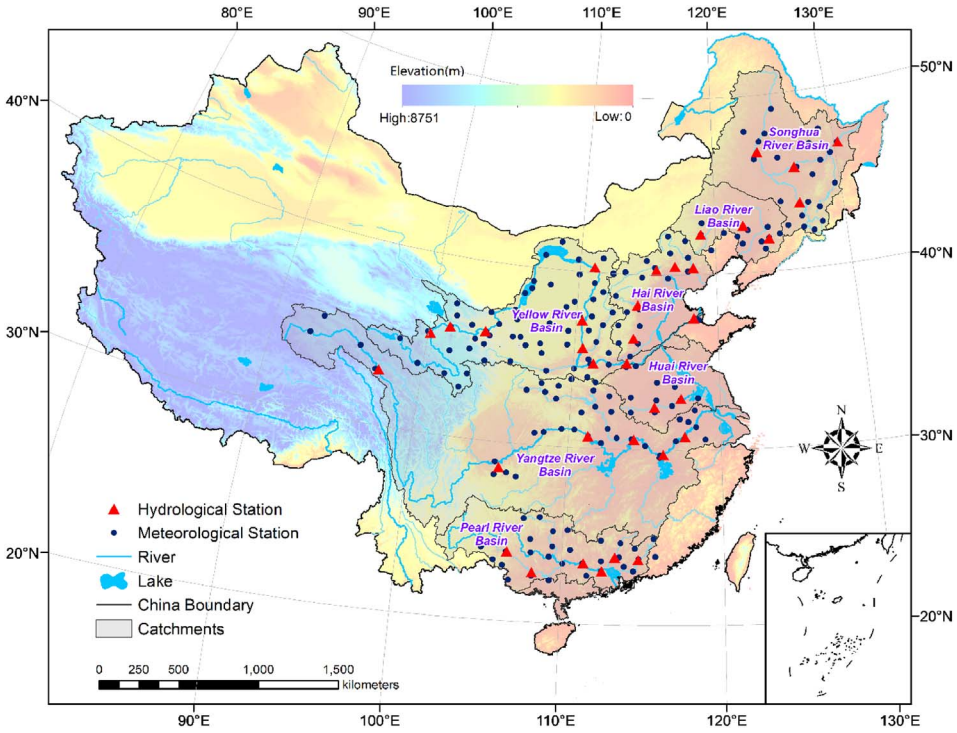

Fig. 2. Location of the seven major basins and the observation stations. Dark blue dots and red triangles represent the meteorological stations and the hydrological stations, respectively. (For interpretation of the references to color in this figure legend, the reader is referred to the web version of this article.)

Table 1
Location information and hydro-climatic characteristics of the 35 catchments used in this study.

Basin	Number	Hydrological station	Longitude	Latitude	Drainage Area	Averaged Annual R	Averaged Annual P	Averaged Annual E_0
			(°E)	(°N)	(km^2)	(mm yr^{-1})	(mm yr^{-1})	(mm yr^{-1})
Songhua River	1	Fengman Reservoir	126.67	43.73	42,500	294.2	695.5	905.0
	2	Jiangqiao	123.69	46.79	162,569	126.4	409.0	1091.3
	3	Harbin	126.58	45.77	389,769	106.4	524.9	1034.5
	4	Jiamusi	130.32	46.8	528,277	121.0	522.6	943.3
Liao River	5	Naodehai Reservoir	122.17	42.68	4051	62.2	523.0	1169.8
	6	Dahuofang Reservoir	124.08	41.88	5437	253.3	790.1	1009.1
	7	Chifeng	118.93	42.28	8678	30.3	371.2	1199.6
Hai River	8	Panjiakou Reservoir	118.3	40.4	33,700	57.5	505.8	1068.7
	9	Miyun Reservoir	116.98	40.47	9027	112.3	579.0	1170.8
	10	Guanting Reservoir	115.6	40.23	42,500	17.3	384.6	1278.4
	11	Huangbizhuang Reservoir	114.3	38.25	23,000	56.9	531.6	1210.9
	12	Guantai	114.08	36.33	17,800	53.5	563.9	1187.6
Yellow River	13	Tangnaihai	100.15	35.5	121,972	171.5	365.7	1001.4
	14	Guide	101.4	36.03	133,650	158.4	252.4	1177.2
	15	Lanzhou	103.82	36.07	222,551	142.4	319.6	1090.5
	16	Hekou	111.07	40.27	367,898	60.8	270.8	1289.0
	17	Baijiachuan	110.42	37.23	29,662	39.4	469.1	1199.4
	18	Longmen	110.58	35.67	497,561	54.6	479.8	1163.8
	19	Sanmenxia	111.37	34.82	688,421	51.5	548.2	1268.7
	20	Huayuankou	113.65	34.92	730,036	53.2	628.3	1271.2
	21	Lijin	118.30	37.53	751,869	41.0	580.0	1362.0
Huai River	22	Wangjiaba	115.60	32.43	30,630	292.5	1021.2	1199.2
	23	Bengbu	117.37	32.95	121,330	211.9	916.3	1203.2
Yangtze River	24	Zhimenda	97.23	33.02	137,704	91.0	482.7	963.0
	25	Chishui	105.68	28.58	16,622	485.1	1135.1	1002.5
	26	Yichang	111.28	30.70	1,005,500	359.3	1149.3	1093.4
	27	Hankou	114.28	30.58	1,488,036	395.8	1246.6	1175.3
	28	Hukou	116.22	29.75	162,225	900.8	1656.0	1148.8
	29	Datong	117.62	30.77	1,705,383	435.1	1375.5	1188.4
Pearl River	30	Baise	106.63	23.90	21,720	1091.7	1324.2	408.8
	31	Nanning	108.23	22.83	72,656	521.6	1312.6	1262.6
	32	Wuzhou	111.33	23.47	327,006	629.9	1479.3	1267.5
	33	Gaoyao	112.47	23.05	351,535	635.2	1654.7	1295.5
	34	Hengshi	113.27	23.85	34,013	1017.1	2180.3	1261.3
	35	Heyuan	114.7	23.73	15,750	942.9	1942.4	1307.6

Table 2
General circulation models used in this study.

Model	Center	Original resolution
BCC-CSM1–1	Beijing Climate Center, China Meteorological Administration	1.125° × 1.125°
GFDL-ESM2M	Geophysical Fluid Dynamics Laboratory	2.5° × 2°
HadGEM2-ES	Met Office Hadley Centre	1.875° × 1.24°
MIROC-ESM-CHEM	Japan Agency for Marine-Earth Science and Technology, Atmosphere and Ocean Research Institute (The University of Tokyo), and National Institute for Environmental Studies	2.8125° × 2.8125°

30-year period in the mid-21st century covering 2040–2069, relative to the reference period of 1961–2000, were forced by four Representative Concentration Pathways (RCP), namely, RCP2.6, RCP4.5, RCP6.0 and RCP8.5.

3. Methodology

3.1. Screening of best fitting Budyko-type equation

With long-standing interest in theoretical aspects of the "Budyko curve", researchers successively proposed numerous forms to improve estimates in local regions and in accounting for different land cover types (Arora, 2002). Table 3 summarizes eight Budyko-type equations proposed by different scholars. Note that various functional forms of the non-parametric and single-parameter Budyko-type equations have been proposed with being validated in different catchments. To quantify the ability of these Budyko-type formulas to reproduce the runoff change of 35 watersheds across China, the history series were divided into the baseline period 1961–1990 and the changed period 1991–2000. Two statistics, the coefficient of determination (R^2) and the mean absolute error (MAE), were used to assess the formulas' performance:

$$R^2 = \left\{ \frac{\sum_{i=1}^{N} (O_i - \overline{O})(S_i - \overline{S})}{\sqrt{\sum_{i=1}^{N} (O_i - \overline{O})^2} \sqrt{\sum_{i=1}^{N} (S_i - \overline{S})^2}} \right\}^2 \quad (1)$$

$$MAE = \frac{\sum_{i=1}^{N} (S_i - O_i)}{N} \quad (2)$$

where, N is the number of time-steps, O and S are the observed and simulated data, $\overline{O}$ and $\overline{S}$ are mean values of the observation and simulation, respectively.

3.2. Climate elasticity method based on Budyko hypothesis

Wang-Tang equation, the latest Budyko-type equation, proposed by Wang and Tang (2014), is assumed to be selected as the favorable functional form. The single parameter, n, in the function can be fitted by:

Table 3
Performance assessment for different Budyko-type equations in runoff change simulation.

Budyko-type equation	Formula	Parameter	R^2	MAE
Schreiber	$E = P[1 - \exp(-E_0/P)]$	Non	0.486	34.35
Ol'dekop	$E = E_0 \tanh(P/E_0)$	Non	0.472	33.01
Turc-Pike	$E = P/[1 + (P/E_0)^2]^{0.5}$	Non	0.479	33.37
Budyko	$E = \{P[1 - \exp(-E_0/P)]E_0 \tanh(P/E_0)\}^{0.5}$	Non	0.480	33.61
Fu	$E = P + E_0 - [P^{n^F} + E_0^{n^F}]^{1/n^F}$	n^F	0.953	5.82
Choudhury	$E = P/[1 + (P/E_0)^{n^C}]^{1/n^C}$	n^C	0.960	5.60
Zhang	$E = P[1 + n^Z(E_0/P)]/[1 + n^Z(E_0/P) + P/E_0]$	n^Z	0.967	5.16
Wang-Tang	$E = \{P + E_0 - [(P + E_0)^2 - 4n^{WT}(2 - n^{WT})PE_0)]^{0.5}\}/[2n^{WT}(2 - n^{WT})]$	n^{WT}	0.998	1.36

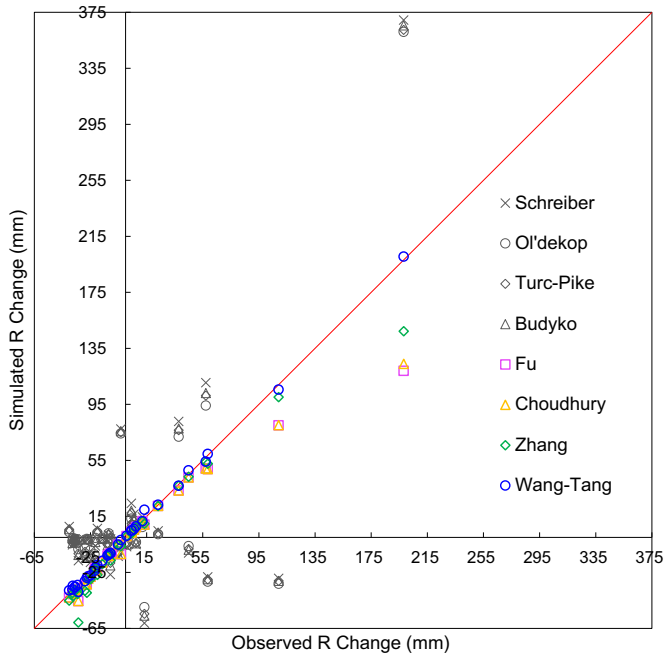

Fig. 3. Comparison of change in runoff estimated by different Budyko-type equations with observed values.

$$E = \frac{P + E_0 - [(P + E_0)^2 - 4n(2 - n)PE_0)]^{0.5}}{2n(2 - n)} \tag{3}$$

Over a long enough time period, the mean annual runoff, Q, can be estimated from the above equations as the difference between mean annual precipitation and mean annual actual evaporation, Q = P-E. Its substitution into Eq. (3) leads to:

$$Q = P - \frac{P + E_0 - [(P + E_0)^2 - 4n(2 - n)PE_0)]^{0.5}}{2n(2 - n)} \tag{4}$$

Assuming P, E_0 and n are independent variables, Eq. (4) can be written as $Q = f(P, E_0, n)$. The first order approximation by total differentiation gives:

$$dQ = \frac{\partial f}{\partial P}dP + \frac{\partial f}{\partial E_0}dE_0 + \frac{\partial f}{\partial n}dn \tag{5}$$

Analogously, Eq. (5) can be derived from any Budyko-type formula listed in Table 3 but without n item for the non-parameter formulas. According to the differentiation form, the simulated dQ can be calculated based on the change in climate variables and catchment characteristics alteration for respective Budyko-type formula.

For the future derivation process, in Eq. (5) $dn = 0$ when no consideration is given to the inter-annual changes in catchment characteristics. Rearranging the terms in Eq. (5), we can have the following form:

$$\frac{dQ}{Q} = \varepsilon_P \frac{dP}{P} + \varepsilon_{E_0} \frac{dE_0}{E_0} \tag{6}$$

where ε_P and ε_{E_0} are the elasticity of runoff with respect to changes in P and E_0, respectively. Here, similar to Schaake (1990) on the precipitation elasticity of runoff, the climate elasticity can be expressed as follows:

$$\varepsilon_P = \frac{\overline{P}}{\overline{Q}}\left(\frac{\partial f}{\partial P}\Big|_{P=\overline{P}, E_0=\overline{E_0}}\right) \tag{7}$$

$$\varepsilon_{E_0} = \frac{\overline{E_0}}{\overline{Q}}\left(\frac{\partial f}{\partial E_0}\Big|_{P=\overline{P}, E_0=\overline{E_0}}\right) \tag{8}$$

where $\overline{Q}$, $\overline{P}$ and $\overline{E_0}$ are the mean annual runoff, precipitation and potential evaporation, respectively. With the respective partial differentials (according to Eq. (4)) given by

$$\frac{\partial f}{\partial P} = 1 - n\frac{2E_0 + 2P + 4E_0n(n - 2)}{4[(E_0 + P)^2 + 4E_0Pn(n - 2)] - 0.5}(n - 2) \tag{9}$$

$$\frac{\partial f}{\partial E_0} = -n\frac{2E_0 + 2P + 4Pn(n - 2)}{4[(E_0 + P)^2 + 4E_0Pn(n - 2)] - 0.5}(n - 2) \tag{10}$$

the elasticities of runoff for the reference period (1961–2000) can be estimated using long-term data of Q, E_0, P and the parameter n for a particular catchment according to Eqs. (7)–(10).

Assuming that the climate elasticities are constant from the history into the future. Thus, changes in mean annual precipitation and potential evaporation can result in projected changes in annual runoff, and the relationship can be approximated as:

$$\frac{\Delta Q}{\overline{Q}} = \varepsilon_P \frac{\Delta P}{\overline{P}} + \varepsilon_{E_0} \frac{\Delta E_0}{\overline{E_0}} \tag{11}$$

3.3. Delta change method

The delta change method was used to compute differences between current and future GCM simulations and add these changes to observed time-series, which is a common method of dealing with GCM inadequacies (Leng and Tang, 2014). As the primary future scenario generation technique, the delta change method is suggested for use in the U.S. National Assessment (see http://www.nacc.usgcrp.gov). Applying the delta change method assumes that GCMs more reliably simulate relative changes rather than absolute values.

In this study, the observed climate data from 1961 to 2000 were employed to derive the 30-yr future climate scenario for the period 2040–2069. It should be noted that the change factors of P and E_0 are distinct. The monthly delta change factors were calculated as follows respectively:

$$Delta(P) = \frac{P_{Gf}}{P_{Gc}} \tag{12}$$

$$Delta(E_0) = E_{0Gf} - E_{0Gc} \tag{13}$$

where the subscript *Gf* and *Gc* respectively indicate the monthly mean

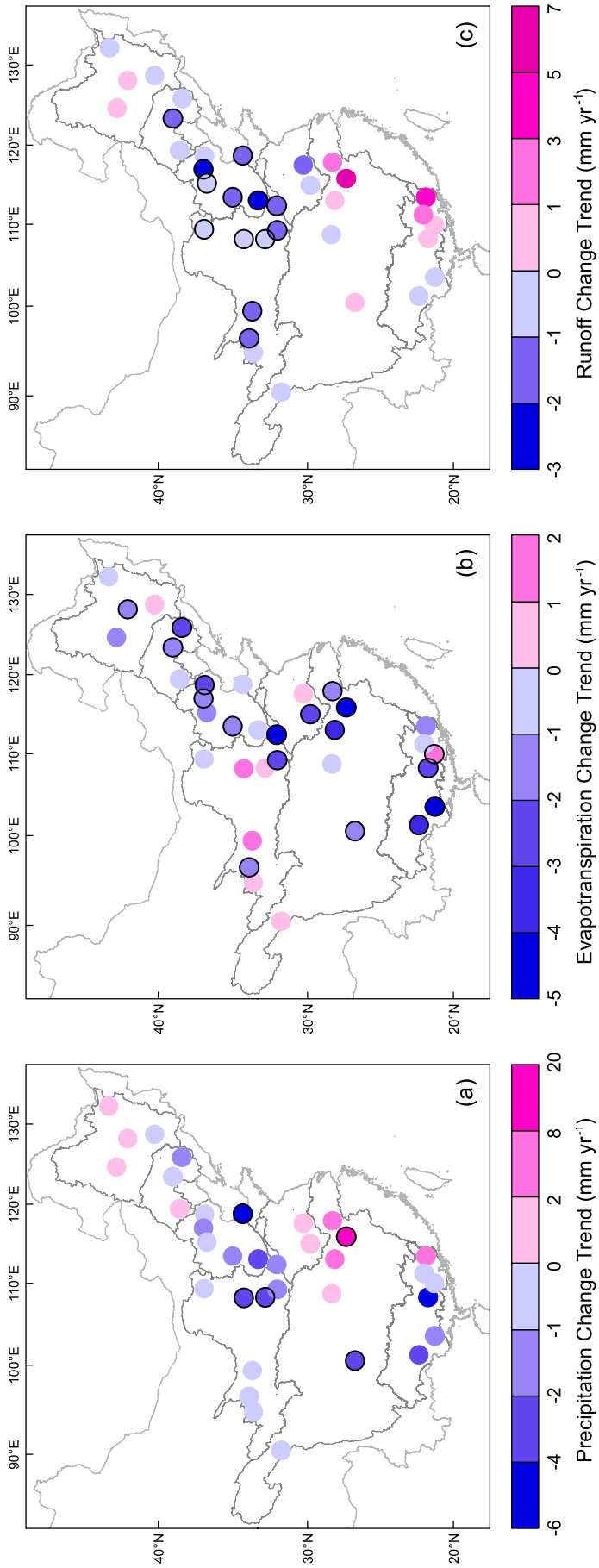

Fig. 4. The changing trends for annual mean (a) precipitation, (b) potential evapotranspiration, and (c) runoff during 1961–2000. Black-edged circles indicate statistical significance at $p = .05$.

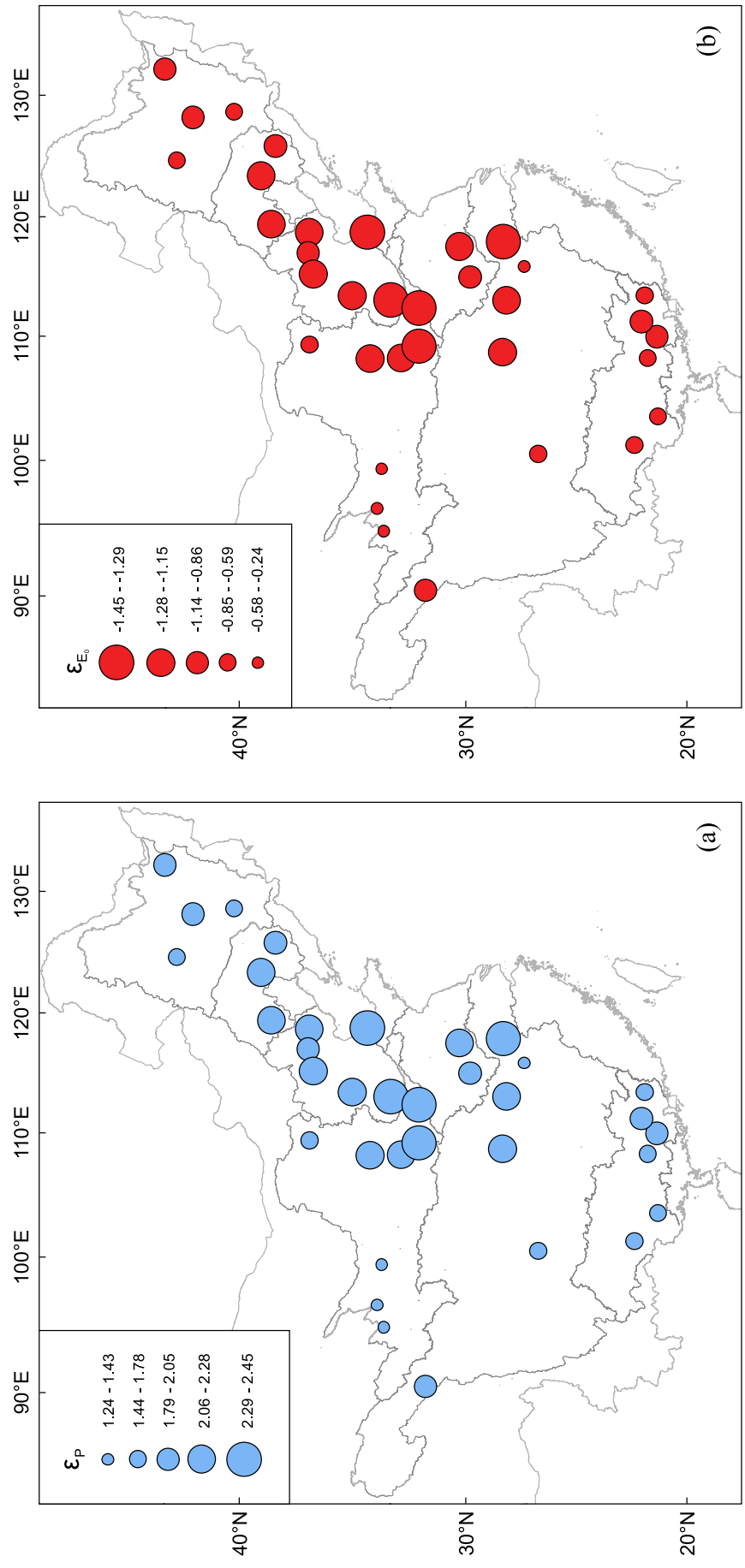

Fig. 5. Elasticity of annual runoff to (a) precipitation and (b) potential evapotranspiration in the 35 catchments.

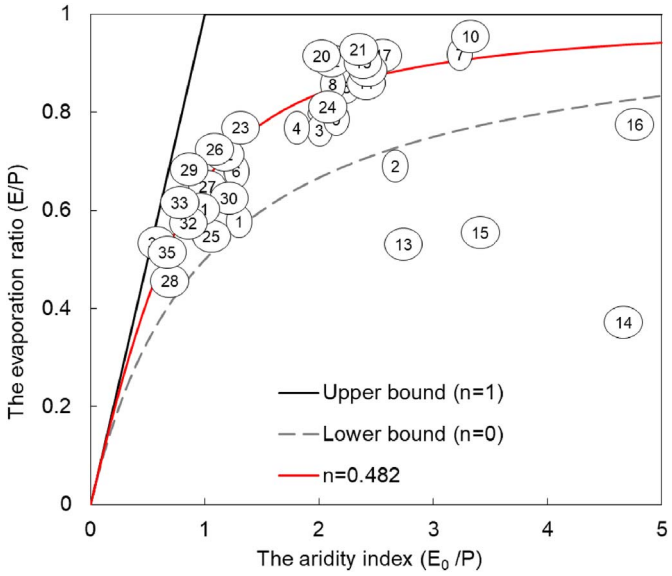

Fig. 6. Distribution of mean annual evaporation ratio (E/P) to mean annual arid index (E_0/P) for 35 catchments.

Table 4
Wang-Tang's *n* values of the 35 catchments.

Basin	Catchment number	Hydrological station	Wang-Tang's n
Songhua River	1	Fengman Reservoir	1.96
	2	Jiangqiao	2.132
	3	Harbin	1.612
	4	Jiamusi	1.637
Liao River	5	Naodehai Reservoir	1.456
	6	Dahuofang Reservoir	1.644
	7	Chifeng	1.473
Hai River	8	Panjiakou Reservoir	1.421
	9	Miyun Reservoir	1.602
	10	Guanting Reservoir	1.342
	11	Huangbizhuang Reservoir	1.431
	12	Guantai	1.373
Yellow River	13	Tangnaihai	2.916
	14	Guide	5.408
	15	Lanzhou	3.034
	16	Hekou	2.22
	17	Baijiachuan	1.405
	18	Longmen	1.472
	19	Sanmenxia	1.401
	20	Huayuankou	1.334
	21	Lijin	1.341
Huai River	22	Wangjiaba	1.509
	23	Bengbu	1.462
Yangtze River	24	Zhimenda	1.582
	25	Chishui	1.636
	26	Yichang	1.418
	27	Hankou	1.416
	28	Hukou	1.996
	29	Datong	1.349
Pearl River	30	Baise	1.75
	31	Nanning	1.627
	32	Wuzhou	1.604
	33	Gaoyao	1.411
	34	Hengshi	1.272
	35	Heyuan	1.539

values for the future and current time periods by GCMs. From this the delta changed future climate variables are formulated as:

$$P_f = P_o \cdot Delta(P) \quad (14)$$

$$E_{0f} = E_{0o} + Delta(E_0) \quad (15)$$

where P_f and E_{0f} are the adjusted future P and E_0 using the delta change method. P_o and E_{0o} are the observed variables in the historical period.

4. Result and discussion

4.1. Optimum Budyko-type equation

The original Budyko formula is entirely deterministic and non-parametric. To incorporate the impact of other factors on water balance, various functional forms, called Budyko-type equations, have been proposed or derived as shown in Table 3. Compared with non-parametric Budyko-type equations, the single-parameter Budyko-type equations have advanced the understanding of the controls of various catchment and climate characteristics, such as vegetation (Li et al., 2013), soil properties (Porporato et al., 2004), seasonality characteristics (Milly, 1994), and topographic controls (Shao et al., 2012). However, many previous studies have chosen the appointed Budyko-type equations to assess the impact of climate change on runoff without statement of convincing proof for their choice. Therefore, in our study, the eight Budyko-type equations have been validated for modeling runoff change to seek out the sole optimal form in runoff projection. Obviously, good agreements can be found for single-parameter Budyko-type equations (i.e., Fu equation, Choudhury equation, Zhang equation, and Wang-Tang equation). Here, Wang-Tang equation (Wang and Tang, 2014) shows the best performance with R^2 and MAE being 0.998 and 1.36 mm, respectively (see Fig. 3 and Table 3). This is expected since the equation has been proved to be flexible to adapt to the catchment characteristics across the study watersheds. The encouraging result also provides confidence in the selection of Wang-Tang equation to project the future runoff change in this study.

4.2. Trends in climatic and hydrologic variables during 1961–2000

The trends of annual P, E_0 and Q series for 35 watersheds were examined using linear regression with the results showing in Fig. 4. Overall, a slightly decreasing trend in annual P has been found, although the trend is not significant at 95% confidence level. There are 24 catchments (i.e., 68.6% of all catchments) showing decreasing trends with four of them the negative trends presenting significant, while the remaining 11 catchments show positive trends in P change with one being significant. Catchments with decreasing trends of P are mostly located in the northern region, particularly in the Hai River Basin and Yellow River Basin (Fig. 4(a)). Significant decreasing trends are detected in E_0 over half of the total watersheds (18 out of the total 35 catchments), only a few catchments show slightly positive trends (6 out of 35 catchments) (Fig. 4(b)). Apparently, mixed increasing and decreasing trends for E_0 can be found in the 35 watersheds, indicating the incoherent and irregular spatial patterns. The significant decreasing trends in annual runoff are detected for the northern regions, including the Yellow River Basin, the Hai River Basin and the Liao River Basin, and slightly increasing trends in the southern regions, including the Yangtze River Basin and the Pearl River Basin (Fig. 4(c)).

4.3. Historical climate elasticity to runoff changes

The climate elasticities of runoff were estimated for 35 catchments based on mean annual hydrometeorological variables according to Eqs. (7)–(10), and the result is shown in Fig. 5. The mean values of P and E_0 elasticities to runoff are 1.972 and −0.972, respectively, indicating a 10% increase in P would increase Q by 19.72% on average, while a 10% increase in E_0 would decrease Q by 9.72% on average. Obviously, runoff changes in these catchments are more sensitive to the temporal variabilities of precipitation (Fig. 5(a)). The P elasticities for the 35 catchments range from 1.24 to 2.45 and the E_0 elasticities range from −1.45 to −0.24. The absolute values of runoff elasticity are relatively high in the Hai River Basin, lower reaches of Yellow River Basin and

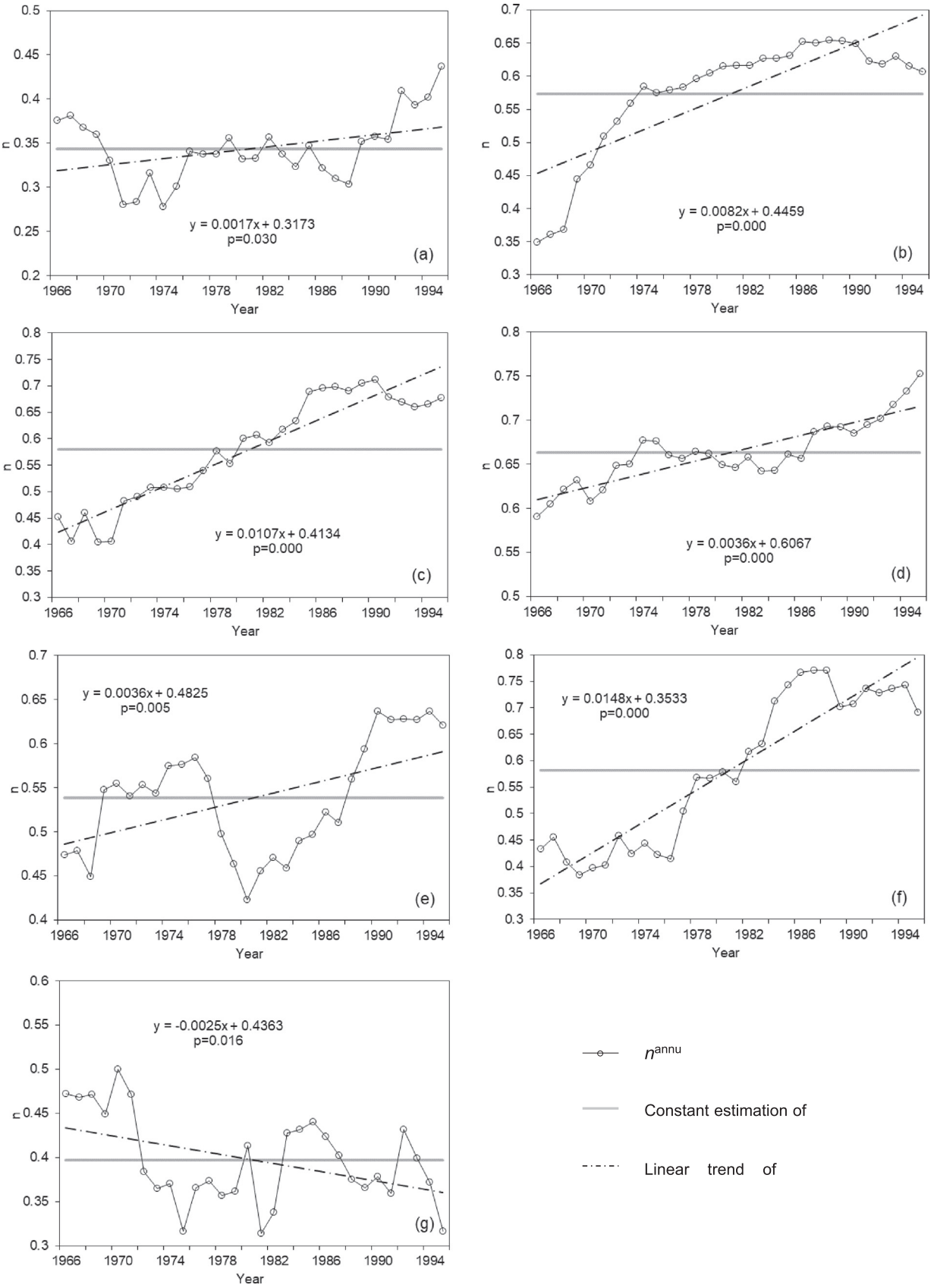

Fig. 7. Evolution and linear trend of the annual parameter n across the seven basins in China ((a): Jiamusi Station on Songhua River Basin; (b): Naodehai Reservoir Station on Liao River Basin; (c): Huangbizhuang Reservoir Station on Hai River Basin; (d): Huayuankou Station on Yellow River Basin; (e): Bengbu Station on Huai River Basin; (f): Hankou Station on Yangtze River Basin and (g): Wuzhou Station on Pearl River Basin). p value is the significance level of the slope of the linear regression.

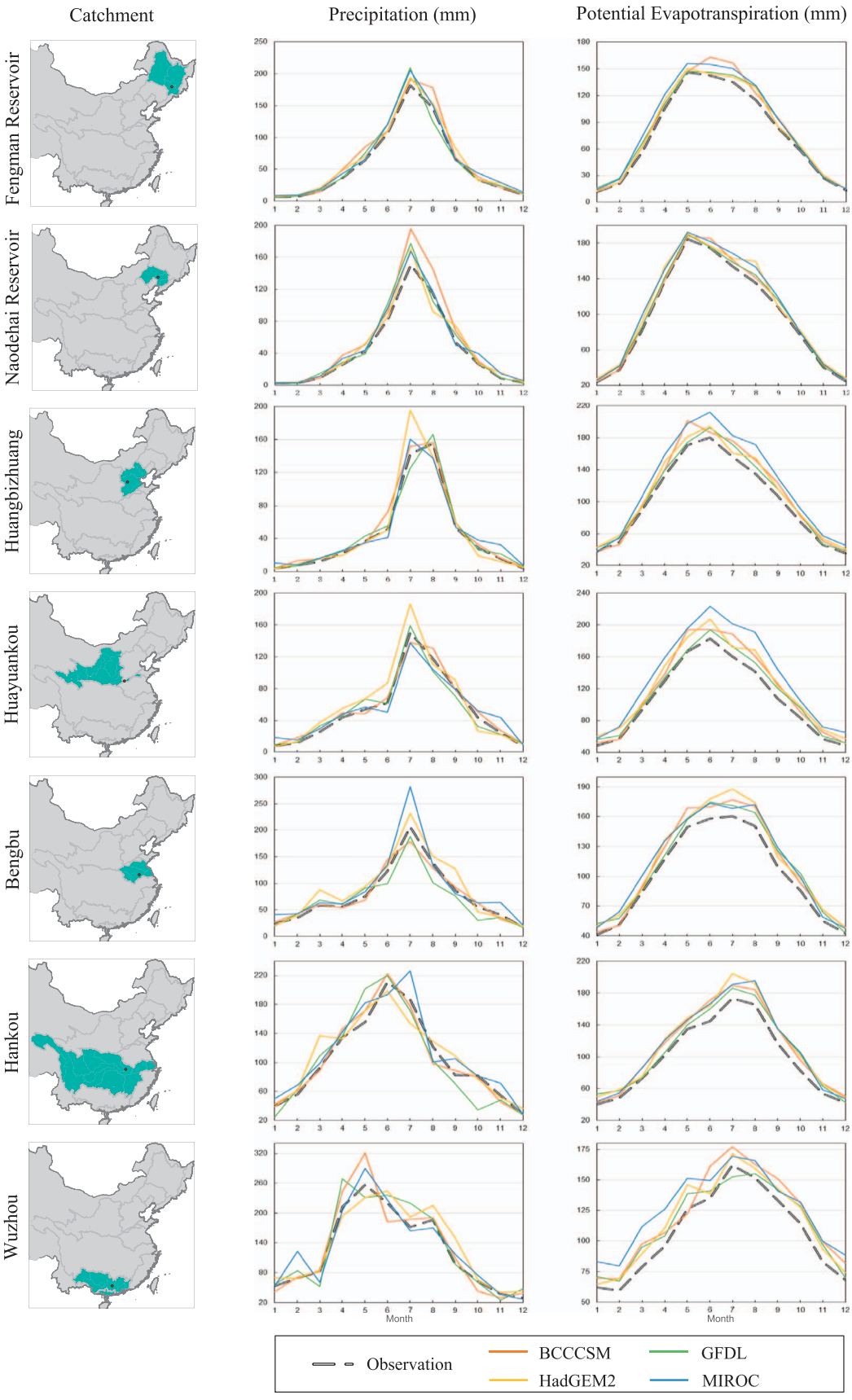

Fig. 8. Monthly mean precipitation and potential evaporation in baseline period and the mid-21st century for RCP4.5 using GCM (Delta change) outputs.

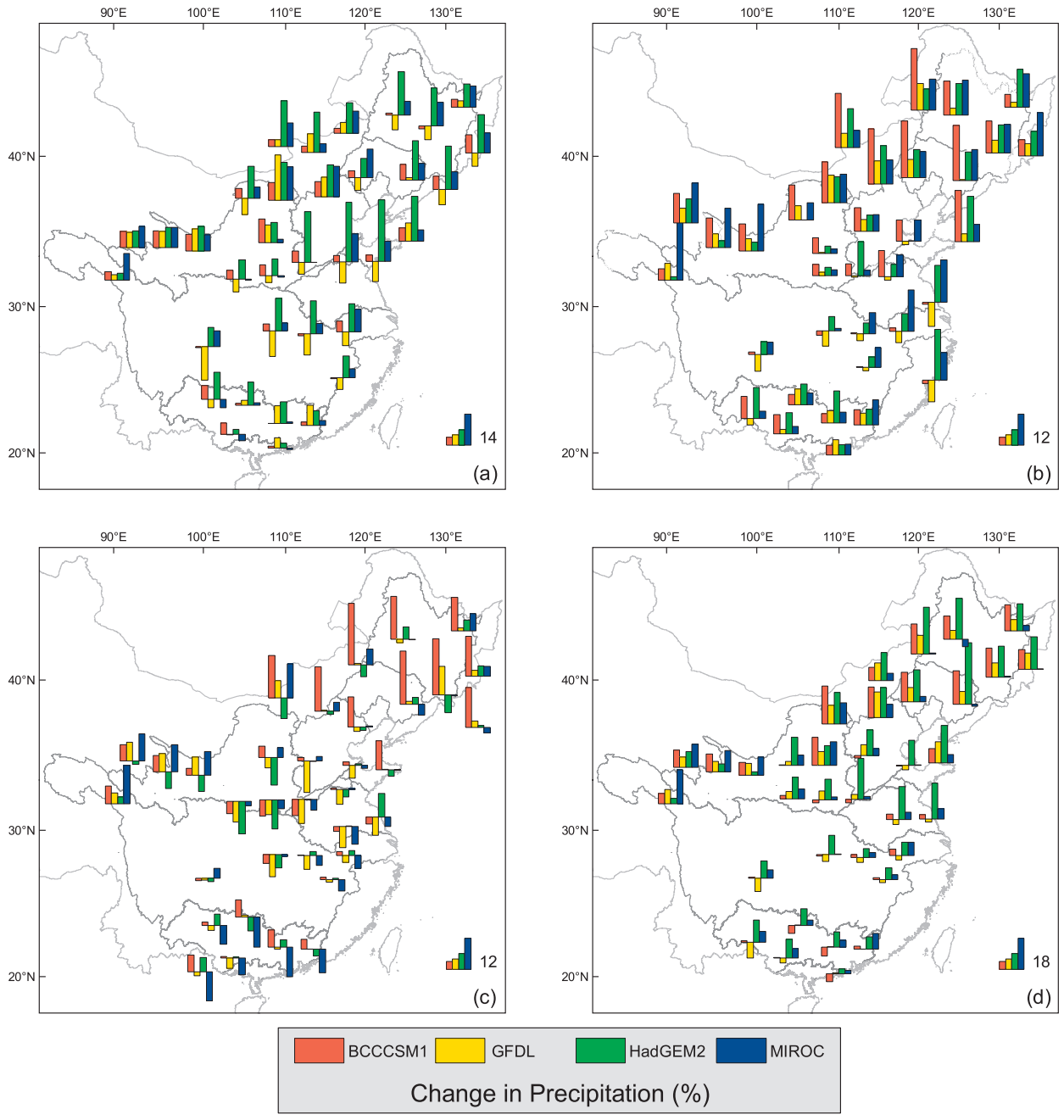

Fig. 9. Relative change of precipitation in the mid-21st century for each RCP (RCP2.6 (a), RCP4.5 (b), RCP6.0 (c), and RCP8.5 (d)).

Yangtze River Basin, indicating that runoff is more sensitive to changes in climate variables in these regions.

In this study, the predictions for the impact of climate change on runoff assume a transition from one steady state to another with no catchment characteristics change. That is, representing the integrated effects of the catchment characteristics, the numerical value of parameter n in the calculation formula (i.e., Eq. (4)) is treated as a constant. However, in practice, the parameter n which can modify the partitioning process of P into E and Q, is probably altered since some of its related factors (e.g., climate, vegetation cover) can be changed over years. Currently, a large variability of n has been revealed at both the global and regional scales by many studies (e.g., Yang et al., 2009; Xiong and Guo, 2012; Li et al., 2013; Jiang et al., 2015, 2017).

In order to properly illustrate the impact of parameter n on the partitioning process of P into E and Q, Fig. 6 presents the distribution of mean evaporation ratio (E/P) as a function of the mean annual arid index (E_0/P) for 35 selected catchments. Note that Eq. (4) can mathematically simulate the domain between the upper bound of the Budyko curve and the horizontal axis (E/P = 0). However, according to the derivation of Wang and Tang (2014), the single parameter n in Wang-Tang equation physical ranges from 0 to 1, since the initial evaporation cannot exceed total evaporation. The majority of the data points are found to accurately satisfy the boundary conditions, except some catchments (scattering in the lower right of the Fig. 6) in the upper reach of the Yellow River Basin, where the extremely drought and cold climate restrain the evapotranspiration. The best-fit curve for these data points achieved by Eq. (4) is when $n = 0.482$, as shown in Fig. 6. Apparently, the lower value of n results in greater runoff under a given climate than the higher value of n. However, small variations of n in extreme wet regions (small aridity index) with narrow boundary controlled by the energy limit are potentially different from same-sized variations of n in extreme dry regions. This phenomenon probably

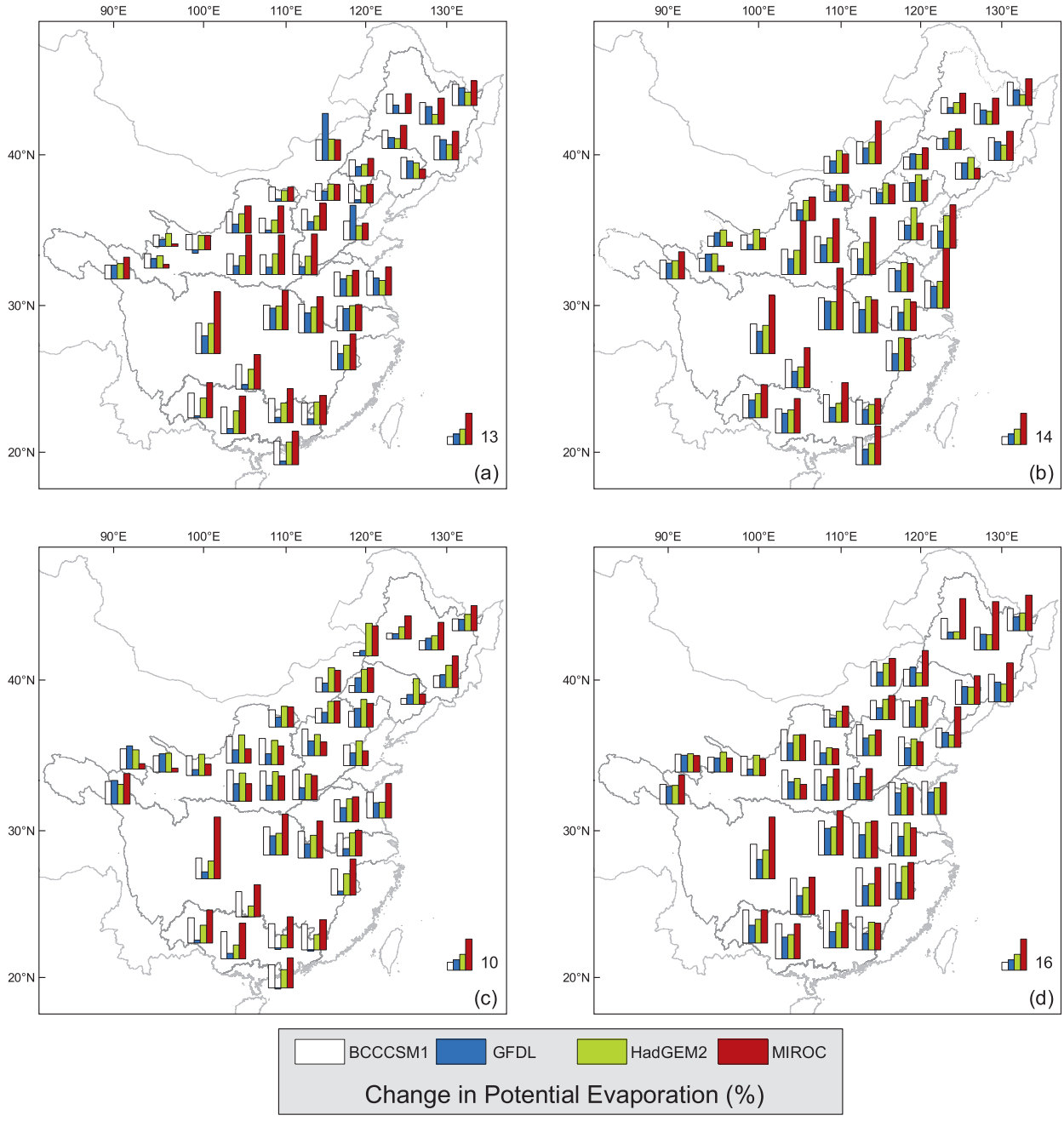

Fig. 10. Same as in Fig. 9, but for the potential evaporation.

suggest that the predictions of runoff are more strongly controlled by n in dry condition than that in very wet condition. This point has been also emphasized in Greve et al. (2015) by introducing a method to evaluate the predictability of water availability that is related to varying catchment characteristics and conditional on the underlying climatic conditions.

Although we have already used respective n values (see Table 4), the key parameter in Budyko curve, to characterize the water energy balance of each catchment, there are still limitations for the assumption due to that n was considered to be influenced by factors which involve a large number of complex processes and interactions and thus cannot keep constant. Recently, Jiang et al. (2015) investigated how the parameters in the Budyko-type equation, would evolve over time by using an 11-year moving window. To further recognize the complexity and irregularity of altering parameter n, the evolution and linear trend of the annual parameter n compared with the estimated value of n treated as a constant are displayed in Fig. 7. It can be seen that the annual parameter n show an irregular fluctuation. All the annual parameters of the seven basins present increasing trends except Wuzhou catchment in Pearl River Basin, which would make the Budyko-type curves moving up. Consequently, for the same hydrological inputs of P and E_0, the evaporation ratio will decrease and the runoff will increase. In our study, the climate elasticity method was employed to reveal the spatiotemporal variations in both historical and future runoff and its key influencing factors in 35 watersheds across China. However, the human interventions, which also an important factor influence the streamflow change, were not considered. Budyko frameworks is based on natural watersheds, meaning that the equations is applicable to a system at steady state (for example, change in water storage is zero). However, there is not so many watersheds that is entirely without human interferences. While anthropogenic factors, as typical time-varying variables, may not be steady over time. More

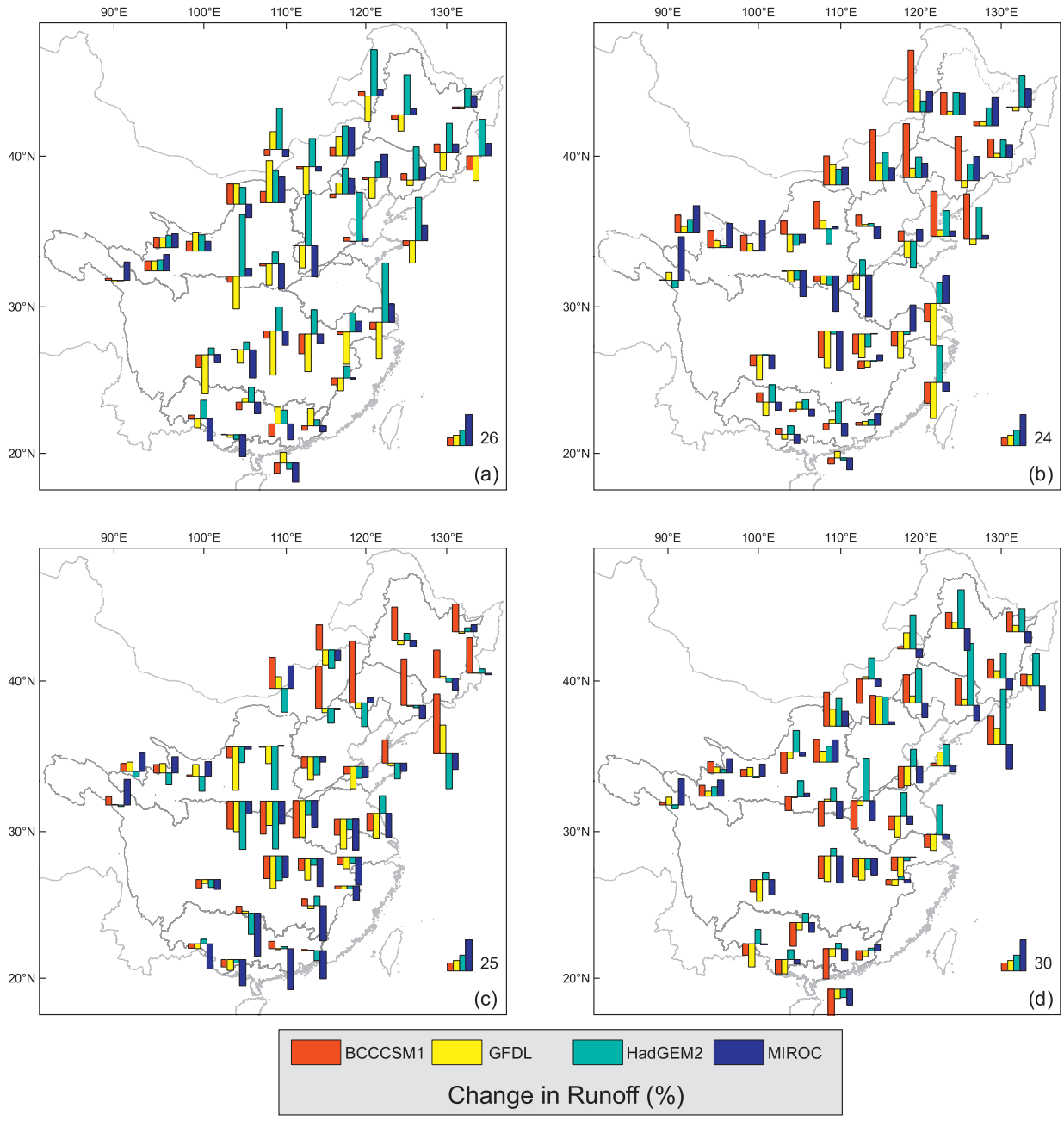

Fig. 11. Same as in Fig. 9, but for the runoff.

importantly, Budyko hypothesis is a theoretical framework, when it applies to a real-life data set, asymmetry from real-life data is likely expected. Due to that the parameter n of each catchment can be influenced by factors which involve a large number of complex processes and interactions (Liang et al., 2015), in the future, the evolution of the Budyko-type equation parameter under the future scenarios considering the changing human interventions should also be considered when predicting accurately the response of runoff to climate change.

4.4. Future climatic variables during mid-21st century

The key advantages of monthly delta change method are the convenient application and the direct scaling of the scenario in line with changes suggested by GCMs. Fig. 8 shows the monthly mean P and E_0 in reference period and the mid-21st century for RCP4.5 using GCMs (by delta change) outputs. Generally, all the results show an increase in both the future P and E_0, although there are a range of discrepancy between the four GCMs predictions.

Fig. 9 shows the spatial distribution of percentage change in the mean annual P by projections from four GCMs. P is projected to increase in the future over large areas of the seven major basins relative to the reference period, especially in parts of northern China, which show lager increments than the southern watersheds. The spatial pattern is very similar for RCP2.6, RCP4.5, and RCP8.5, but the largest positive growth always occurs on RCP8.5. The main negative anomalies of precipitation are found over southeast region in RCP6.0, such as Huai River Basin, lower Yellow River and lower Yangtze River Basins. The regions with larger increased precipitation are the semi-arid and semi-humid climate zones of China (Liu et al., 2017). In Huang et al. (2011)'s study, the change of annual mean precipitation in the Yangtze River basin would present a trend of deficit precipitation in 2020s; insignificant changes in the 2050s; and a surplus of precipitation in the 2080s

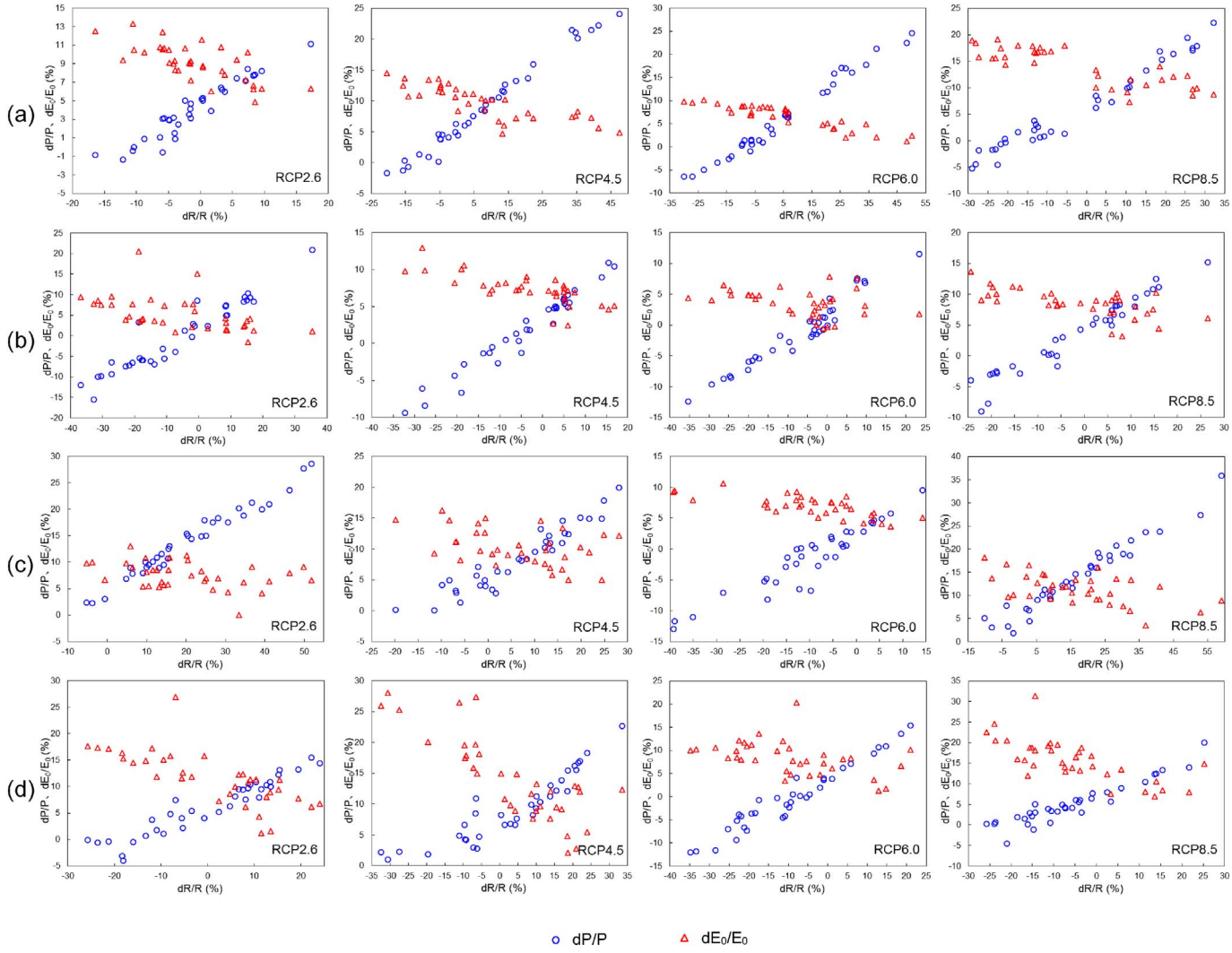

Fig. 12. Relative runoff change related with precipitation and potential evapotranspiration changes in the future scenarios for four GCMs ((a) BCCCSM1; (b) GFDL; (c) HadGEM2 and (d) MIROC).

as compared to the mean values of the reference period. Overall, in our study, the relative change rates of annual mean precipitation over seven major basins in the mid-21st century are 14%, 12%, 12%, and 18% for RCP2.6, RCP4.5, RCP6.0, and RCP8.5, respectively.

Accordingly, the projected changes in E_0 relative to the reference period in the mid-21st century are depicted in Fig. 10. Results show positive changes in mean annual E_0 over the entire study area for all four RCPs. Meanwhile, a larger magnitude of E_0 changes can be found in the southeast regions than the northwest regions. Generally, the growth rates of E_0 increased with the effect of emission scenarios with values of 13%, 14%, 10%, and 16% for RCP2.6, RCP4.5, RCP6.0, and RCP8.5, respectively. The continuous increase in E_0 in the 21st century was also revealed by climate models across both the Tibetan Plateau and Haihe River Basin (Wang et al., 2013b; Xing et al., 2014).

4.5. Mean annual runoff changes in mid-21st

The results for mean annual runoff changes in mid-21st modeled by Eq. (11) with four GCMs outputs, are presented in Fig. 11. It can be seen that there are huge distinction in the mean annual runoff change projections between both GCMs and RCPs. Fig. 11 (a) shows that under RCP2.6 the mean annual runoff of almost all watersheds will increase in mid-21st by HadGEM2 model, but will decrease by GFDL model. Positive changes in the north and negative changes in the south of China can be practically generalized from the majority of GCMs projections under RCP4.5 and RCP8.5 (Fig. 11(b) and Fig. 11(d)). W5hile under RCP6.0, the future mean annual runoff of all the watersheds locating on the south of Yellow River will experience a decreasing trend (Fig. 11(c)). Overall, increasing trends in the future mean annual runoff will occur in the northern China, and the decreasing trends will happen in the southern China. Compared with that in the reference period, runoff will change by −11.1-23.5% for RCP2.6, −20.4-22.0% for RCP4.5, −26.1-8.6% for RCP6.0 and −16.1-22.1% for RCP8.5 on average, respectively. This phenomenon of runoff decline was also identified in southeast and far southwest Australia, although there is no clear agreement between the global climate models in the direction of future precipitation and runoff change (Teng et al., 2012). In China, Zhang et al. (2015) found that the average streamflow in the Hexi Corridor of Northwest China would increase by 10.5 to 22.0% during 2021 to 2050. A 12.8% increase in streamflow was projected during 2021 to 2050 in the Heihe catchment (Zhang et al., 2016a). Xu et al. (2009) projected streamflow change in the headwater catchment of the Yellow River Basin by using the SWAT model and found the decreasing trend in annual streamflow in 2010–2099. Our results are largely consistent to the reported in the literatures.

In fact, as shown in Fig. 12, a certain range in the projection of precipitation change, which is usually larger than that of potential evaporation, can be found in diverse future scenarios and GCMs. We

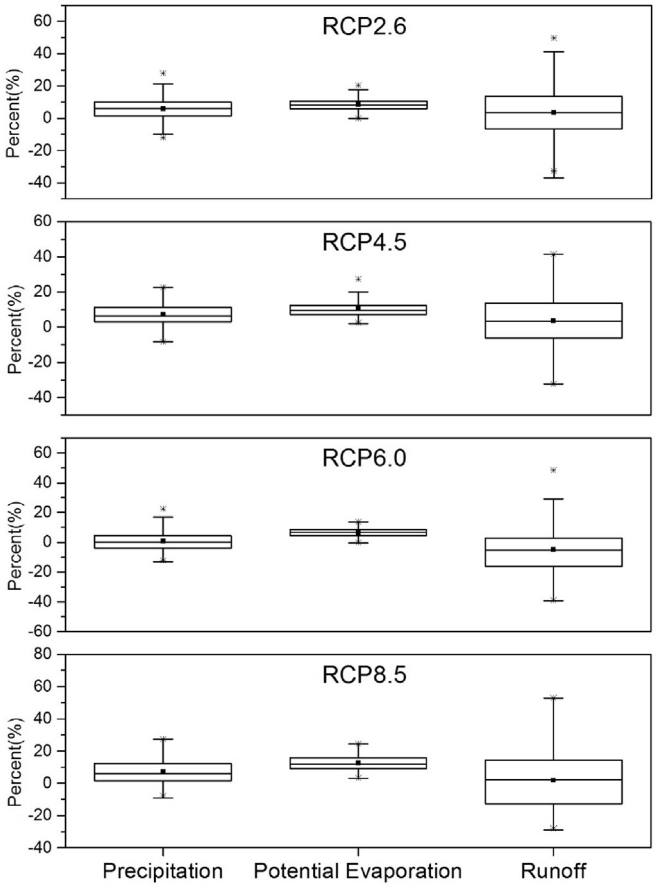

Fig. 13. Predicted relative changes in precipitation, potential evaporation, and runoff over seven major basins of China in the mid-21st century for each RCP. The median and mean values of the predicted changes are shown as lines and black dots insides the boxes; the box indicates the 25th–75th percentile range; whiskers extend to the 5th and 95th percentiles; and stars represent the 1st and 99th percentiles.

can still sort out a clear linear relationship between relative change in runoff and precipitation. Hence, it is evident that the effect of precipitation on runoff change is more significant than that of potential evaporation, that is, precipitation is the main driver of runoff change in the projections. Precipitation as a dominant factor affecting runoff change was also found in Yangtze River Basins by Guo et al. (2015).

Furthermore, the range of results are summarized in Fig. 13, showing the 5th, 25th, 75th, 95th percentile, median and mean values of the predicted changes. It is worth noting that the range of E_0 changes is much smaller than that of P and Q, even the predicted percentage change in E_0 is a bit larger than changes in P and Q, and all the values in E_0 change are positive. The percentage change of runoff shows complex tendency. As shown in Fig. 13, there is a large uncertainty in the future projections with the GCMs disagreeing even on the direction of runoff change across most of the catchments, the spatial patterns of mean annual runoff change are generally similar under all the RCPs, except for RCP2.6, under which pathway the negative and positive changes in runoff occurring at some catchments are nearly offset. Nevertheless, there is consistency in the most GCM projections for RCP4.5 and RCP8.5, where practically the results show an increase in the future runoff over northern basins and a decline over southern basins, respectively. Here, the negative changes in runoff are mainly due to a larger increase in E_0 compared with P. In addition, a larger magnitude of changes in runoff have been found with the greenhouse gas increases, the largest change rate always occurs under RCP85 with a mean of 30%.

Although the future runoff change predicted by four GCMs under four different RCPs with the delta change method, it is worth noting that there are still uncertainties associated with the projection of runoff change. Firstly, as presented by many researches, the largest uncertainty of climate projection and related impact assessment often comes from GCMs due to model structures (Prudhomme and Davies, 2009; Vetter et al., 2017). Since daily series of climate predictors are provided by plenty of GCMs, only four GCMs were driven in this study, which can bring unavoidable uncertainty. It is difficult to give a definite variation even a direction of change on climate based on such few GCMs. The second uncertainty is from the scaling methods. Downscaling large-scale predictors to generate future precipitation and potential evaporation based on multiple linear regression, the major focus on delta change method is still whether the temporal sequencing of wet and dry days for the present climate are stationary in the future, which is always a weak point of the method that is hard to be confirmed. Overall, the projection of climatic and hydrologic variables with comprehensive consideration of these uncertainties is an area of active and ongoing research.

5. Conclusion

To accurately predict the future runoff change induced by climate change, and avoid the complexity and uncertainty from model structure and parameterization of conventional hydrological models, a two-parameter climate elasticity method based on Budyko-type equation was proposed in this study. The proposed method was applied to project the spatiotemporal variations in future runoff and its key influencing factors in 35 catchments of seven major basins with different climate types across China. In summary, the research results highlight the following:

1. Compared with the non-parametric Budyko-type equation, the single-parameter Budyko-type equations are more flexible to adapt to different catchment characteristics. Based on the ability of multiform Budyko-type equations in reproducing the runoff change, Wang-Tang equation, which is proved to be the most effective formula in modeling runoff change across our study watersheds, was selected as the optimal Budyko equation to assess the impacts of climate change on historical and future runoff.
2. Although slightly and significantly decreasing trends in precipitation and potential evaporation occurred in the majority of catchments, respectively, there are richer spatial patterns of annual trends in precipitation and potential evaporation during the period of 1961–2000. The annual runoff presents significant decreasing trends in the northern and increasing trends in the southern regions of the study area, respectively. Results of climate elasticity analysis between annual runoff and climatic variables show that runoff is more sensitive to climatic variables in the Hai River Basin and lower Yellow River Basin.
3. For future climate scenarios generating from four corrected GCMs outputs, precipitation is projected to increase over large areas of the seven major basins relative to the reference period, especially in parts of northern basins, which showing lager increase than southern catchments. Concurrently, positive changes in mean annual potential evaporation can be found over the entire study area for all four RCPs. The effect of precipitation on runoff change is more significant than that of potential evaporation, that is, precipitation is the main driver of runoff in the projection results. The projected relative changes in runoff series show complex tendency. Nevertheless, an increasing trend in the north and a decreasing in the south can be generalized from the majority of GCMs outputs.

Acknowledgements

This work was jointly supported by the National Science Foundation of China (51779073, 51379057), the Fundamental Research Funds for the Central Universities (2017B21414), the National “Ten Thousand Program” Youth Talent, and the Six talent peaks project in Jiangsu

Province. Thanks to the National Meteorological Information Center, China Meteorological Administration (http://cdc.cma.gov.cn) for offering the meteorological data and also thanks to the Working Group of the World Climate Research Program on Coupled Modeling, which is responsible for CMIP5. Cordial thanks are extended to the Editor, Professor Liviu Matenco, and two anonymous reviewers for their critical and constructive comments which highly improve the quality of the manuscript.

References

Arora, V.K., 2002. The use of the aridity index to assess climate change effect on annual runoff. J. Hydrol. 265, 164–177. http://dx.doi.org/10.1016/S0022-1694(02)00101-4.

Berghuijs, W., Woods, R., Hrachowitz, M., 2014. A precipitation shift from snow towards rain leads to a decrease in streamflow. Nat. Clim. Chang. http://dx.doi.org/10.1038/NCLIMATE2246.

Budyko, M.I., 1974. Climate and Life, English ed. Academic, San Diego, Calif.

China Ministry of Water Resources, 2009. China Water Resources Bulletin 2009. China Water Power Press.

Choudhury, B.J., 1999. Evaluation of an empirical equation for annual evaporation using field observations and results from a biophysical model. J. Hydrol. 216, 99–110.

Donohue, R.J., Roderick, M.L., McVicar, T.R., 2012. Roots, storms and soil pores: incorporating key ecohydrological processes into Budyko's hydrological model. J. Hydrol. 436, 35–50.

Greve, P., Gudmundsson, L., Orlowsky, B., Seneviratne, S.I., 2015. Introducing a probabilistic Budyko framework. Geophys. Res. Lett. 42, 2261–2269. http://dx.doi.org/10.1002/2015GL063449.

Guo, S., Guo, J., Hou, Y., Xiong, L., Hong, X., 2015. Prediction of future runoff change based on Budyko hypothesis in Yangtze River basin. Adv. Water Sci. 26, 151–160 (In Chinese with English abstract).

Huang, J., Zhang, J., Zhang, Z., CY, Xu, Wang, B., Yao, J., 2011. Estimation of future precipitation change in the Yangtze River basin by using statistical downscaling method. Stoch. Env. Res. Risk A. 25 (6), 781–792. http://dx.doi.org/10.1007/s00477-010-0441-9.

Huang, Z., Yang, H., Yang, D., 2016. Dominant climatic factors driving annual runoff changes at the catchment scale across China. Hydrol. Earth Syst. Sci. 20 (7), 2573–2587.

IPCC, 2013. Summary for policymakers. In: Working Group I Contribution to the IPCC Fifth Assessment Report Climate Change 2013: The Physical Science Basis. Cambridge Univ. Press, Cambridge, UK.

Jiang, C., Xiong, L., Wang, D., Liu, P., Guo, S., CY, Xu, 2015. Separating the impacts of climate change and human activities on runoff using the Budyko-type equations with time-varying parameters. J. Hydrol. 522, 326–338.

Jiang, C., Xiong, L., Guo, S., Xia, J., CY, Xu, 2017. A process-based insight into non-stationarity of the probability distribution of annual runoff. Water Resour. Res. 53. http://dx.doi.org/10.1002/2016WR019863.

Kumar, S., Zwiers, F., Dirmeyer, P.A., Lawrence, D.M., Shrestha, R., Werner, A.T., 2016. Terrestrial contribution to the heterogeneity in hydrological changes under global warming. Water Resour. Res. 52, 3127–3142. http://dx.doi.org/10.1002/2016WR018607.

Leng, G., Tang, Q., 2014. Modeling the impacts of future climate change on irrigation over China: sensitivity to adjusted projections. J. Hydrometeorol. 15 (15), 2085–2103.

Li, D., Pan, M., Cong, Z., Zhang, L., Wood, E., 2013. Vegetation control on water and energy balance within the Budyko framework. Water Resour. Res. 49 (2), 969–976. http://dx.doi.org/10.1002/wrcr.20107.

Liang, W., Bai, D., Wang, F., Fu, B., Yan, J., Wang, S., Yang, Y., Long, D., Feng, M., 2015. Quantifying the impacts of climate change and ecological restoration on streamflow changes based on a Budyko hydrological model in China's Loess Plateau. Water Resour. Res. 51, 6500–6519. http://dx.doi.org/10.1002/2014WR016589.

Liu, Q., McVicar, T.R., 2012. Assessing climate change induced modification of Penman potential evaporation and runoff sensitivity in a large water-limited basin. J. Hydrol. 464–465, 352–362. http://dx.doi.org/10.1016/j.jhydrol.2012.07.032.

Liu, J., Zhang, Q., Zhang, Y., Chen, X., Li, J., Aryal, S.K., 2017. Deducing climatic elasticity to assess projected climate change impacts on streamflow change across China. J. Geophys. Res. 122, 10228–10245. http://dx.doi.org/10.1002/2017JD026701.

Meng, D., Mo, X., 2012. Assessing the effect of climate change on mean annual runoff in the Songhua River basin, China. Hydrol. Process. 26, 1050–1061. http://dx.doi.org/10.1002/hyp.8180.

Milly, P.C.D., 1994. Climate, soil water storage, and the average annual water balance. Water Resour. Res. 30, 2143–2156. http://dx.doi.org/10.1029/94WR00586.

Mishra, V., Cherkauer, K.A., Shukla, S., 2010. Assessment of drought due to historic climate variability and projected future climate change in the Midwestern United States. J. Hydrometeorol. 11 (1), 46–68.

Penman, H.L., 1948. Natural evaporation from open water, bare soil and grass. Proc. R. Soc. London, Ser. A 193 (1032), 120–145.

Porporato, A., Daly, E., Rodriguez-Iturbe, I., 2004. Soil water balance and ecosystem response to climate change. Am. Nat. 164 (5), 625–632.

Prudhomme, C., Davies, H., 2009. Assessing uncertainties in climate change impact analyses on the river flow regimes in the UK. Part 1: baseline climate. Clim. Chang. 93 (1), 177–195.

Renner, M., Seppelt, R., Bernhofer, C., 2012. Evaluation of water-energy balance frameworks to predict the sensitivity of streamflow to climate change. Hydrol. Earth Syst. Sci. 16 (5), 1419–1433. http://dx.doi.org/10.5194/hess-16-1419-2012.

Roderick, M.L., Farquhar, G.D., 2011. A simple framework for relating variations in runoff to variations in climatic conditions and catchment properties. Water Resour. Res. 47, W00G07. http://dx.doi.org/10.1029/2010WR009826.

Schaake, J.C., 1990. From climate to flow. In: Waggoner, P.E. (Ed.), Climate Change and U.S. Water Resources. John Wiley, New York, pp. 177–206 chap. 8.

Shao, Q., Traylen, A., Zhang, L., 2012. Nonparametric method for estimating the effects of climatic and catchment characteristics on mean annual evapotranspiration. Water Resour. Res. 48, W03517. http://dx.doi.org/10.1029/2010WR009610.

Singh, R., Kumar, R., 2015. Vulnerability of water availability in India due to climate change: a bottom-up probabilistic Budyko analysis. Geophys. Res. Lett. 42, 9799–9807.

Sun, Y., Zhang, X., Ren, G., Zwiers, F.W., Hu, T., 2016. Contribution of urbanization to warming in China. Nat. Clim. Chang. http://dx.doi.org/10.1038/NCLIMATE2956.

Teng, J., Chiew, F.H.S., Vaze, J., Marvanek, S., Kirono, D.G.C., 2012. Estimation of climate change impact on mean annual runoff across continental Australia using Budyko and Fu equations and hydrological models. J. Hydrometeorol. 13, 1094–1106.

Thompson, J.R., Green, A.J., Kingston, D.G., Gosling, S.N., 2013. Assessment of uncertainty in river flow projections for the Mekong River using multiple GCMs and hydrological models. J. Hydrol. 486 (4), 1–30.

Vetter, T., Reinhardt, J., Flörke, M., et al., 2017. Evaluation of sources of uncertainty in projected hydrological changes under climate change in 12 large-scale river basins. Clim. Chang. 141 (3), 419–433. http://dx.doi.org/10.1007/s10584-016-1794-y.

Wang, D., Tang, Y., 2014. A one-parameter Budyko model for water balance captures emergent behavior in Darwinian hydrologic models. Geophys. Res. Lett. 41, 4569–4577. http://dx.doi.org/10.1002/2014GL060509.

Wang, W., Shao, Q., Yang, T., Peng, S., Xing, W., Sun, F., Luo, Y., 2013a. Quantitative assessment of the impact of climate variability and human activities on runoff changes: a case study in four catchments of the Haihe River basin, China. Hydrol. Process. 27, 1158–1174. http://dx.doi.org/10.1002/hyp.9299.

Wang, W., Xing, W., Shao, Q., Yu, Z., Peng, S., Yang, T., Yong, B., Taylor, J., Singh, V.P., 2013b. Changes in reference evapotranspiration across the Tibetan Plateau: observations and future projections based on statistical downscaling. J. Geophys. Res. 118, 1–20.

Wang, W., Zou, S., Shao, Q., Xing, W., Chen, X., Jiao, X., Luo, Y., Yong, B., Yu, Z., 2016. The analytical derivation of multiple elasticities of runoff to climate change and catchment characteristics alteration. J. Hydrol. 541, 1042–1056.

Williams, C.A., Reichstein, M., Buchmann, N., Baldocchi, D., Beer, C., Schwalm, C., Wohlfahrt, G., Hasler, N., Bernhofer, C., Foken, T., Papale, D., Schymanski, S., Schaefer, K., 2012. Climate and vegetation controls on the surface water balance: synthesis of evapotranspiration measured across a global network of flux towers. Water Resour. Res. 48, W06523. http://dx.doi.org/10.1029/2011WR011586.

Wu, Y., Wu, S., Wen, J., Xu, M., Tan, J., 2016. Changing characteristics of precipitation in China during 1960–2012. Int. J. Climatol. 36, 1387–1402.

Xing, W., Wang, W., Shao, Q., Peng, S., Yu, Z., Yong, B., Taylor, J., 2014. Changes of reference evapotranspiration in the Haihe River Basin: present observations and future projection from climatic variables through Multi-model ensemble. Glob. Planet. Chang. 115, 1–15. http://dx.doi.org/10.1080/02626667.2016.1170132.

Xing, W., Wang, W., Shao, Q., Yu, Z., Yang, T., Fu, J., 2016. Periodic fluctuation of reference evapotranspiration during the past five decades: does Evaporation Paradox really exist in China? Sci. Rep. 6, 39503. http://dx.doi.org/10.1038/srep39503.

Xiong, L., Guo, S., 2012. Appraisal of Budyko formula in calculating long-term water balance in humid watersheds of southern China. Hydrol. Process. 26, 1370–1378.

Xu, Z., Zhao, F., Li, J., 2009. Response of streamflow to climate change in the headwater catchment of the Yellow River basin. Quat. Int. 208 (1), 62–75. http://dx.doi.org/10.1016/j.quaint.2008.09.001.

Xu, X., Liu, W., Scanlon, B.R., Zhang, L., Pan, M., 2013. Local and global factors controlling water-energy balances within the Budyko framework. Geophys. Res. Lett. 40, 6123–6129. http://dx.doi.org/10.1002/2013GL058324.

Yang, H., Yang, D., 2011. Derivation of climate elasticity of runoff to assess the effects of climate change on annual runoff. Water Resour. Res. 47, W07526. http://dx.doi.org/10.1029/2010WR009287.

Yang, D., Shao, W., Yeh, P.J.F., Yang, H., Kanae, S., Oki, T., 2009. Impact of vegetation coverage on regional water balance in the nonhumid regions of China. Water Resour. Res. 45, W00A14. http://dx.doi.org/10.1029/2008WR006948.

Yin, Y., Ma, D., Wu, S., Pan, T., 2015. Projections of aridity and its regional variability over China in the mid-21st century. Int. J. Climatol. 35, 4387–4398. http://dx.doi.org/10.1002/joc.4295.

Zhang, Q., Gu, X., Singh, V.P., CY, Xu, Kong, D., Xiao, M., Chen, X., 2015. Homogenization of precipitation and flow regimes across China: changing properties, causes and implications. J. Hydrol. 530, 462–475.

Zhang, A., Liu, W., Yin, Z., Fu, G., Zheng, C., 2016a. How will climate change affect the water availability in the Heihe River Basin, Northwest China? J. Hydrometeorol. 17 (5), 1517–1542.

Zhang, S., Yang, H., Yang, D., Jayawardena, A.W., 2016b. Quantifing the effect of vegetation change on the regional water balance within the Budyko framework. Geophys. Res. Lett. 43, 1140–1148. http://dx.doi.org/10.1002/2015GL066952.